

Ergodic Boundary in Numerical Simulations of Two-Dimensional Turbulence

G. S. Deem and N. J. Zabusky

Bell Telephone Laboratories, Whippany, New Jersey 07981

(Received 14 June 1971)

In numerical calculations, we observe a dichotomy in the time evolution of solutions of the high-Reynolds-number, two-dimensional, incompressible Navier-Stokes equations using power-law initial modal energy spectra $E(\kappa, 0) \sim \kappa^{-\mu_0}$. The boundary is expressed in terms of critical values of viscosity ν_{cr} and microscale λ_{cr} . For both parameters initially above critical, μ approaches 4. For both parameters initially below critical, μ approaches 1 at large κ , consistent with equipartition of the *vorticity* spectrum. In the former case, large-scale vortex states form after a long time; and, in both cases, energy flows to the lowest wave numbers.

The incompressible Navier-Stokes equations in two dimensions have attracted increasing interest in recent years because of their relevance in studies of atmospheric predictability.^{1,2} Insights obtained will also help our understanding of three-dimensional turbulence. Two- and three-dimensional turbulence phenomena are amenable to similar analytical treatments, but only in the former environment can we perform high-resolution numerical experiments and learn synergetically.^{3,4}

Kraichnan,⁵ Leith,⁶ and Batchelor⁷ have given theoretical and reasonable phenomenological arguments for the existence of a temporally asymptotic inertial range spectrum

$$E(\kappa, t) = \bar{\beta}(t)\kappa^{-\mu}, \quad (1)$$

where $\mu = 3$ and $E(\kappa, t)$ is the scalar modal energy spectrum, related to the total fluid energy by

$$\langle u^2(t) \rangle = \frac{1}{2} \langle \tilde{u} \cdot \tilde{u} \rangle = \int_0^\infty E(\kappa, t) d\kappa; \quad (2)$$

here $\tilde{u} = (u, v)$ and κ , the scalar wave number, is $2\pi k/L_x$, with $k = 1, 2, \dots, \frac{1}{2}N$ the integer mode number and L_x the periodic interval in one direction.

Lilly^{8,9} studied numerically the *vorticity* representation of the two-dimensional (2D) Navier-Stokes equations on an $N \times N$ doubly periodic lattice with $N = 64$. Lilly interprets his results as consistent with $\mu = 3$.

We have obtained higher-resolution solutions of the primitive Navier-Stokes equations,

$$\partial_t u + u \partial_x u + v \partial_y u = -\partial_x p + \nu \nabla^2 u, \quad (3a)$$

$$\partial_t v + u \partial_x v + v \partial_y v = -\partial_y p + \nu \nabla^2 v, \quad (3b)$$

$$\partial_x u + \partial_y v = 0; \quad (3c)$$

and our results differ from Lilly's, as shown in case 1, Table I. The results of case 2 show a

TABLE I. Two-dimensional spectral power coefficients for the inertial range (doubly periodic lattice, $N = 128$; 64 wave numbers).

	Initial ($t = 0$)		Final	
	μ	k region	μ	k region
Case 1	4	$2 \leq k \leq 64$	4	$1 \leq k \leq 40$
Case 2	2.5	$4 \leq k \leq 64$	2.5	$2 \leq k < 14$
			1	$14 < k \leq 64$

very different behavior, discussed below.

The results of case 1 are consistent with recent theoretical-phenomenological studies by Chorin¹⁰ and Saffman.¹¹ The latter predicts an equilibrium inertial range of 4. We have also observed a $\mu = 4$ spectrum in the fine-scale structure of a two-dimensional inviscid shear flow.⁴

We solve (3) using a second-order finite-difference algorithm¹² that "semiconserves" energy and enforces the finite-difference analog of (3c) at each time step. We apply periodic boundary conditions on the unit square $L_x \times L_y = 1 \times 1$. We construct the initial velocity field from a modal representation of the stream function ψ which has random phases and yields a power-law spectrum for $E(\kappa, 0)$ in a certain range of κ (see Table I). We construct $E(\kappa, t)$ from the full two-dimensional modal energy spectrum $E(\kappa_x, \kappa_y, t)$ by integrating around circular bands in the $\kappa_x - \kappa_y$ plane. Table II gives properties of the initial and final states of cases 1 and 2. Angular brackets indicate spatial averages over (x, y) ; and, unless otherwise specified, *all* quantities are time dependent.

Figure 1 shows temporal variations of $\langle u^2 \rangle$, enstrophy $\langle \omega^2 \rangle$,⁸ microscale

$$\lambda(\tau) = [\langle u^2 \rangle / \langle \partial_x u \rangle^2]^{1/2}, \quad (4)$$

TABLE II. Properties of solutions on a 128x128 periodic lattice.

Case	Normalized time τ	$\nu \times 10^4$	$10^{-3} \times R_\lambda$	Time step	Integral scale L^a	Microscale λ	Circulation time (time steps)
1	0	1.363	1.0	0	0.1818	0.1363	100
1	9.5	1.363	2.443	950	0.4570	0.3425	258
2	0	0.2974	1.0	0	0.05357	0.02974	50
2	11.0	0.2974	0.790	550	0.1350	0.02552	137

Normalized time τ	Total energy	Mode-4 energy	Mode-40 energy	Mode-64 energy	$\langle \omega^2 \rangle$	$-\langle u^2 \rangle^{-1} d\langle u^2 \rangle / dt$
0	1.0000	3.302×10^{-2}	2.300×10^{-6}	2.972×10^{-7}	390.6	0.05325
9.5	0.9460	8.305×10^{-3}	2.379×10^{-7}	2.071×10^{-8}	128.5	0.008701
0	1.0000	0.2500	9.849×10^{-4}	2.567×10^{-4}	8413	0.2503
11.0	0.8480	0.1120	1.389×10^{-3}	9.677×10^{-4}	8429	0.2956

^a L and λ are to be compared with 1.0, the periodicity interval.

integral scale

$$L(\tau) = \frac{1}{4} \int \langle u(x, y)u(x+r, y) + v(x, y)v(x, y+r) \rangle \times d\tau / \langle u^2 \rangle, \quad (5)$$

and Reynolds number $R_\lambda(\tau) = \langle u^2 \rangle^{1/2} \lambda / \nu$. Note that u in the denominator of (4) and u and v in (5) are velocity components obtained from (3). We

interpret the integral in (5) in discrete form as a sum over displacements $x+r$ and $y+r$ about points (x, y) . Cases 1 and 2 are approximately the same duration when time is normalized with initial circulation time according to $\tau \equiv [\langle u^2(0) \rangle^{1/2} / L(0)] t \equiv [\langle u_0^2 \rangle^{1/2} / L_0] t$.

Figure 2 shows log-log plots of $E(\kappa, \tau) / \lambda \langle u^2 \rangle$ versus $\kappa \lambda$ at particular times. Table I is the re-

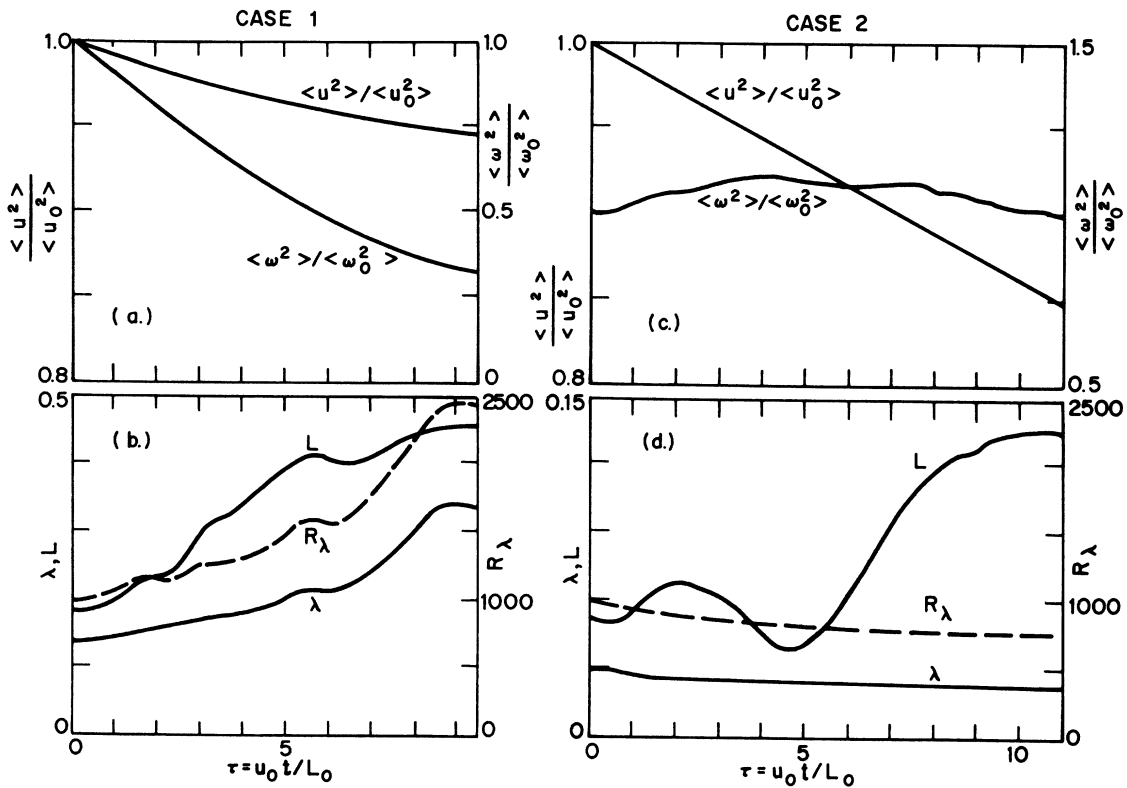


FIG. 1. Time variation of mean-square velocity, enstrophy, microscale, integral scale, and Reynolds number R_λ for cases 1 and 2.

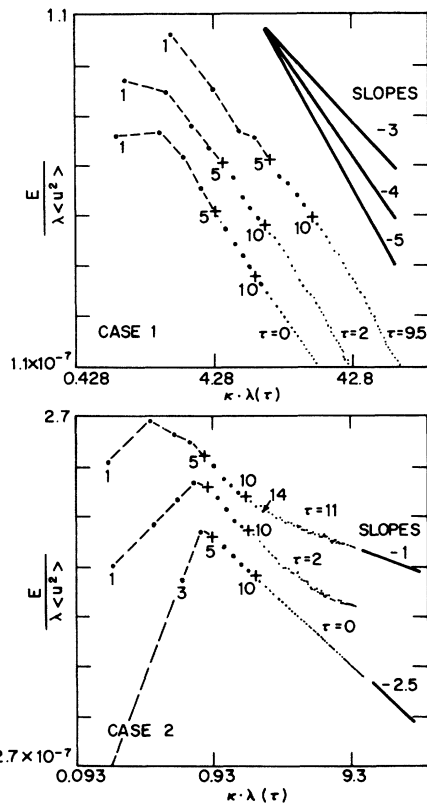


FIG. 2. Log-log plots of normalized modal energy spectra versus $\kappa\lambda(\tau)$ for cases 1 and 2. In each case, the spectra at the particular times $\tau \equiv (\langle u_0^2 \rangle^{1/2} / L_0) t = 0, 2$ are displaced downwards two decades and one decade, respectively. Modes 6 and higher are shown as unconnected dots. The dots represent computer output at a specific time, that is, they are unaveraged.

sult of performing short-time averages over spectra such as those in Fig. 2. The κ^{-4} spectrum of Fig. 2(a) is approximately stationary in time. The late-time, large- κ^{-1} energy spectrum of Fig. 2(b) corresponds to an enstrophy spectrum linear in κ , or a near equipartition of the vorticity spectrum. Thus, we have identified an "ergodic" or "stochastic" boundary for high-Reynolds-number, two-dimensional numerical turbulence depending upon the initial parameters, for example the viscosity and distribution of modal energies. Such boundaries have been predicted on the basis of heuristic analyses and have been applied to nonlinear lattices in one dimension¹³ and to other physical systems.¹⁴ In observing movies of $E(\kappa, t)$, one sees small fluctuations propagate toward higher wave numbers and energy feed slowly into the lowest wave numbers.

The differences in the two cases are evident in

the time variation of λ and R_λ . In Fig. 1(b), they both increase (as does the integral scale); in Fig. 1(d), they both decrease slightly (the integral scale continues to increase on the average, as a result of energy coupling to low wave numbers). The initial increase in $\langle \omega^2 \rangle$ in Fig. 1(c) is the result of a competition between generation due to truncation errors and decay due to viscosity [evident in Fig. 1(a)].

The increase of the $k = 1$ modal energy for case 1, evident in Fig. 2, corresponds in physical space to a slow coalescence of smaller vortices into a pair of counter-rotating, large-scale vortices. At late times, these vortices "trap" Lagrangian particles.¹⁵ In case 2, the flow remains significantly less structured although, at late times, large-scale features are evident (growth of low modes in Fig. 2).

Giorgini and Travis,¹⁶ using a Fourier modal representation with 64×64 modes, studied 2D Navier-Stokes turbulence starting with $R_\lambda \approx 1500$ and $\nu \approx 10^{-4}$ (compare with case-2 parameters). Their results show a turn-up in the high- κ end of the spectrum (see their Fig. 4), which we interpret as incipient vorticity equipartition. In three dimensions energy equipartition is expected for the truncated continuum problem¹⁷ where viscosity becomes infinite for $\kappa > \kappa_{max}$ ($= N\pi$).

Our results are consistent with a boundary in the λ - ν plane. For case 1, we have $\lambda > \lambda_{cr}$ and $\nu > \nu_{cr}$, and for case 2, $\lambda < \lambda_{cr}$ and $\nu < \nu_{cr}$. If $\lambda > \lambda_{cr}$ and $\nu < \nu_{cr}$, we conjecture that the high end of the spectrum will show a κ^{-1} behavior at very long times. Case 2 and the Giorgini and Travis results give evidence that this boundary is a property of the truncated continuum 2D Navier-Stokes equations and is not due to a specific numerical algorithm and its associated aliasing properties.

¹E. N. Lorenz, *Tellus* **21**, 3 (1969).

²J. Smagorinsky, K. Miyakoda, and R. F. Strickler, *Tellus* **22**, 2 (1970).

³N. J. Zabusky, in *Nonlinear Partial Differential Equations*, edited by W. Ames (Academic, New York, 1966).

⁴N. J. Zabusky and G. S. Deem, *J. Fluid Mech.* **47**, 353 (1971).

⁵R. Kraichnan, *Phys. Fluids* **10**, 1417 (1967).

⁶C. E. Leith, *Phys. Fluids* **11**, 671 (1968).

⁷G. K. Batchelor, *Phys. Fluids*, Suppl. II, 233 (1969).

⁸D. K. Lilly, *Phys. Fluids*, Suppl. II, 240 (1969).

⁹D. K. Lilly, *J. Fluid Mech.* **45**, 395 (1971).

¹⁰A. J. Chorin, "Turbulence Spectra, Equilibrium and

Vortex Formation" (to be published).

¹¹P. G. Saffman, "A Note On the Spectrum and Decay of Random Two-Dimensional Vorticity Distributions at Large Reynolds Number" (to be published).

¹²The numerical algorithm used to solve 3(a)–3(c) is described in Ref. 4, with the exception that the duFort-Frankel treatment of viscous terms is replaced by a forward differencing in the present paper. The accuracy of the algorithm is second order for small viscosity ν .

¹³F. M. Izrailev and B. V. Chirikov, Dokl. Akad. Nauk SSSR **166**, 57 (1966) [Sov. Phys. Dokl. **11**, 30 (1966)]; B. V. Chirikov, in Proceedings of the International Con-

gress of Mathematicians, Moscow, 1966 (unpublished).

¹⁴G. M. Zaslavskii, *Statistical Irreversibility of Non-linear Systems* (Science Publishing House, Moscow, 1970) (in Russian).

¹⁵G. S. Deem, N. J. Zabusky, R. H. Hardin, and F. D. Tappert, to be published.

¹⁶A. Giorgini and J. R. Travis, in Proceedings of the Symposium on Stochastic Hydraulics, University of Pittsburgh, Pittsburgh, Pa., 1971 (to be published).

¹⁷T. D. Lee, Quart. Appl. Math. **10**, 69 (1952). We have observed energy equipartition in numerical simulations of the Taylor-Green problem for zero viscosity on a $32 \times 32 \times 32$ mesh.

Plasma Diffusion Due to Weak Nonaxisymmetry*

Chuan Shen Liu

Gulf General Atomic Company, San Diego, California 92212, and University of California, Los Angeles, Los Angeles, California 90024

(Received 14 June 1971)

Plasma diffusion due to static, nonaxisymmetric perturbations of magnetic or electric field is analyzed in the low collision-frequency region. The diffusion coefficient is found to be proportional to the fraction of the particles with slow drift, and can significantly exceed classical diffusion.

In the dc octopole experiments, the plasma diffusion has two distinctive stages.¹ In the first stage, when the plasma density is sufficiently high, the density is inversely proportional to time with constant density profile. The diffusion coefficient is essentially classical, proportional to the collision frequency and, therefore, to density. Subsequently, when the density becomes very low, the plasma decays exponentially in time, indicating a diffusion coefficient independent of density. This nonclassical diffusion cannot be attributed to plasma turbulence, as no fluctuation of sufficient amplitude has been observed, and has thus remained a mystery. Recently, Ohkawa² suggested that the magnetic field error could be important to the diffusion process by inducing random walk across the magnetic surface. In this Letter, the plasma diffusion due to the breaking of the axisymmetry by the static magnetic and electric perturbations is studied in the low-density region, where the collision frequency is lower than the average bounce (transit) frequency of the electrons. The diffusion coefficient $D_{\Psi} \sim \Delta(\delta v_{\Psi})^2 \tau$ has the following characteristics: (i) The random-walk velocity (δv_{Ψ}) is given by the radial drift velocity due to the non-axisymmetric field perturbation, while the random-walk frequency is given by the average drift in the unperturbed state across the characteris-

tic scale length of the field perturbation. (ii) It is independent of the plasma density, but depends on the fraction of the particles with slow drift velocity Δ , which contribute dominantly to diffusion. (iii) The radial electric field is critical for its existence.

Consider a plasma in an axisymmetric poloidal field given by $B = \Delta \Psi \times \Delta \theta$, where Ψ is the flux function and θ the azimuthal angle. In the guiding-center approximation, the particle dynamics consists of three quasiperiodic motions with distinctive frequencies³: gyration around the magnetic field with gyrofrequency $\Omega = qB/Mc$; bounce (transit) along the field line with bounce (transit) frequency $\nu_b = [\oint ds/v_{\parallel}]^{-1}$; and drift across the field line with drift frequency $\omega_d \sim \epsilon \nu_b \sim \epsilon^2 \Omega$, where $\epsilon \ll 1$ is the ratio of gyroradius to the characteristic scale length of the magnetic field. The corresponding adiabatic invariants are $\mu = \frac{1}{2} M v_{\perp}^2 / B$, $J = \oint ds M v_{\parallel}$, and $A = \oint \Psi d\theta$. In the absence of nonaxisymmetric perturbation, the particle drift is along θ , deviating from a given magnetic flux surface Ψ only by the order of gyroradius. The nonaxisymmetric perturbation, either magnetic or electrostatic, renders it possible for the particles to drift across the Ψ surface, which is also the constant-density surface for a Maxwellian plasma. In the presence of collisions these drifts lead to a random walk along the density